Arch. Metall. Mater. **65** (2020), 2, 793-797

DOI: 10.24425/amm.2020.132822

M. JĘDRUSIK[1,2*], Ł. CIENIEK[1], A. KOPIA[1], CH. TURQUAT[2], CH. LEROUX[2]

STRUCTURAL CHARACTERIZATION OF $LaCoO_3$ THIN FILMS GROWN BY PULSED LASER DEPOSITION

Thin films of crystallized $LaCoO_3$ were grown on Si substrate by Pulsed Laser Deposition at different temperatures (750°C, 850°C and 1000°C). The structural characterization of the $LaCoO_3$ thin films was done by combining several techniques: Scanning Electron Microscopy (SEM), Atomic Force Microscope (AFM), Transmission Electron Microscopy (TEM) and Grazing Incidence X-Ray Diffraction (GIXRD). The thin films crystallized in the expected rhombohedral phase whatever the deposition temperature, with an increase of crystallite size from 70 nm at 750°C to 100 nm at 1000°C, and an average thickness of the thin films of less than 200 nm. At 850°C and 1000°C, the thin films are crack-free, and with a lower number of droplets than the film deposited at 750°C. The grains of $LaCoO_3$ film deposited at 850°C are columnar, with a triangular termination. At 1000°C, an intermediate layer of $La_2Si_2O_7$ was observed, indicating diffusion of Si into the deposited film.

Keywords: PLD, thin films, perovskites, $LaCoO_3$

1. Introduction

Perovskites ABO_3 have attracted the interest of researchers because it is a promising class of materials especially in the electronic industry, due to their electrical conductivity properties [1-4]. But these materials are also popular as sensing medium in gas detection devices because of their high thermal stability and good catalytic properties [5-8]. $LaCoO_3$ has been established as a promising material for resistive sensors [9], electrochemical sensors [10], temperature sensors [11], as well as catalysts and photocatalysts [12]. These perovskites have very good catalytic properties in the presence of gases such as CO, NO_x, and H_2S [13-15].

$LaCoO_3$ based sensors in the form of thin films were recently tested for CO detection [16]. The films showed a high response, excellent recovery and good stability to CO gas at low-temperature T = 200°C. $LaCoO_3$ nanoparticles with the perovskite-type structure were successfully synthesized by Ortiz et al. [17]. The $LaCoO_3$ pellets presented a high sensitivity for both CO and C_3H_8 at different concentrations and operating temperatures.

Various preparation methods are reported for the synthesis of $LaCoO_3$ thin films or powders like sol-gel, CVD, PVD or PLD [18-21]. All these methods and their parameters influence the structural morphology, phase or chemical composition and hence the properties of the material. In case of thin films for gas sensors, the morphology of the surface of the thin films, the grain size and crystallographic orientation, as well as the exposed facets influenced the response time and sensitivity to the gas of interest. Grains in the nanometer range result in a higher reactive surface and higher sensitivity of the gas sensor. The surface state is also important as was stated by Say et al [14] in their comparative study of the perfect and the oxygen defective $LaCoO_3$ (001) surfaces.

The aim of this primary work on the synthesis of $LaCoO_3$ thin films by Pulsed Laser Deposition (PLD) was to investigate the influence of process temperature on the morphology and crystallographic structure of the obtained thin films deposited on silicon (Si) substrates in presence of oxygen

2. Methodology

The $LaCoO_3$ (99,9%) target (diameter = 2,5 cm) was purchased from the Kurt J. Lesker Company. The thin films were deposited on (100) oriented Si substrates purchased from the

[1] AGH UNIVERSITY OF SCIENCE AND TECHNOLOGY, DEPARTMENT OF SURFACE ENGINEERING AND MATERIALS CHARACTERISATION, FACULTY OF METALS ENGINEERING AND INDUSTRIAL COMPUTER SCIENCE, AL. A. MICKIEWICZA 30, 30-059 KRAKOW, POLAND
[2] UNIVERSITÉ DE TOULON, AMU, CNRS, IM2NP, CS 60584, TOULON, F-83041, FRANCE

* Corresponding author: jedrusik@agh.edu.pl

SurfaceNet GmbH (10×10 mm, Ra < 0,5 nm) using a laser ablation system equipped with a Nd-YAG (λ = 266 nm) laser and a Neocera chamber, in presence of oxygen (40 mTorr), at 3 different substrate temperatures 750°C, 850°C and 1000°C. The deposition conditions were a laser pulse frequency of 10 Hz, and energy density on the target of 7.8 J/cm^2, a laser pulse duration of 4 ns and a deposition time fixed at 2.5 hours. The phase analyses of the thin films were performed by means of the X-ray diffraction method using PAN analytical EMPYREAN DY 1061 equipped with a Cu Kα tube, in Bragg-Brentano geometry and grazing angles of 1° and 3°. The X rays diffraction patterns were refined using the software MAUD and cif files. The morphology of the thin films were studied by SEM using a Zeiss Supra 40, and by TEM, using a Tecnai G2 operating at 200 kV, on cross-sectional samples, prepared in a conventional way, through mechanical thinning followed by low angles ion milling. The film roughness was analyzed by AFM using a Veeco Dimension® Icon™ SPM with the NanoScope V instrument.

3. Results and discussion

The XRD pattern are presented Fig. 1. The corresponding depth of penetration is z = 54 nm. The identification of phases was assessed thanks to the JCPDS database, specifically the card numbers 04-009-4883. The three diffractions patterns correspond to the expected rhombohedral phase for $LaCoO_3$. The peak intensity changes with the temperature of the substrate, with (012) being the most intense peak for T = 750°C to (110) being the most intense one for T = 850°C and T = 1000°C, in the 2θ range 20-40°. However, determining the preferred orientation (texture analysis) is not straightforward due to the changes in the reflection vector q in grazing geometry compared to Bragg Brentano geometry [22].

Cell parameters, angle α (°), cell volume, and reliability factors (weighted profile R-factor – Rwp, expected R factor – $Rexp$), deduced from the X rays diffraction patterns refinements, are given in Table 1.

TABLE 1

Cell parameters, volume cell, and refinement R factors

Sample	a (Å)	α (°)	V (Å^3)	$Rexp$ / Rwp
$LaCoO_3$-750	5.4199	60.72	114.41	4.32/6.79
$LaCoO_3$-850	5.3971	60.69	112.90	6.90/10.56
$LaCoO_3$-1000	5.3979	60.67	112.90	6.25/9.16

The cell parameter as well the α angle slightly decreases with increasing deposition temperature. This can be linked to the presence of cobalt vacancies in the layers [23].

The surface morphology of thin films is of great importance in the case of gas sensing applications because the crystallographic facets exposed to the gas may govern the detection properties. Fig. 2 shows SEM images of the surface morphology for the different layers. The $LaCoO_3$-750 layer is characterized

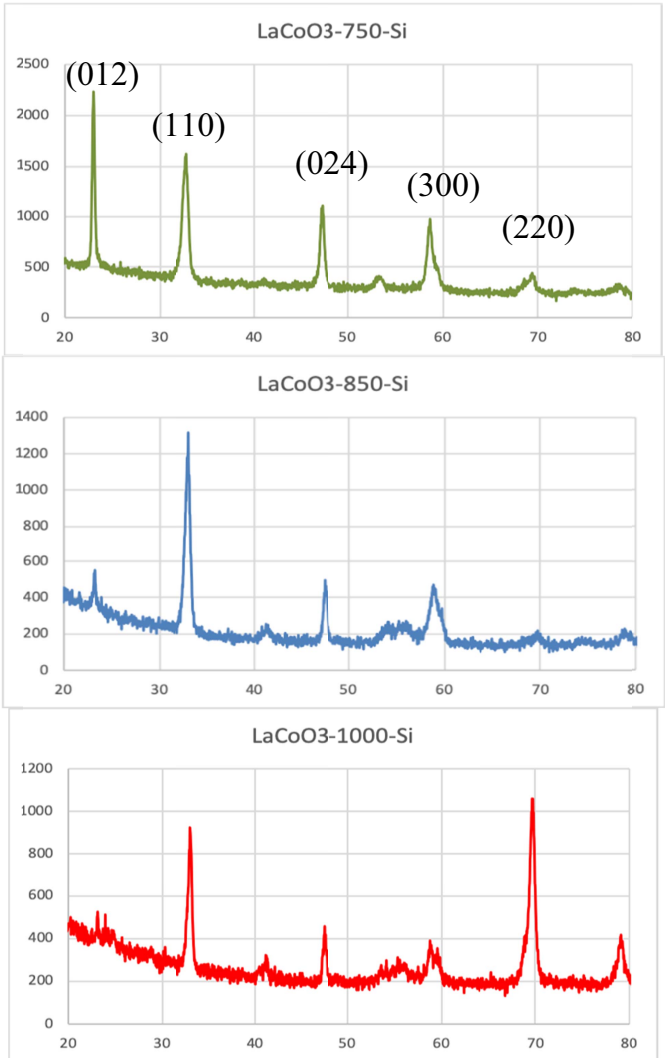

Fig. 1. XRD patterns of $LaCoO_3$ thin films

by the presence of cracks and a big number of droplets (Fig. 2a). The mean grain size is around 70 nm. The $LaCoO_3$-850 layer (Fig. 2b) shows an interesting specific morphology, with triangular grains and a flat termination and a small number of droplets. This grain shape is consistent with a $[111]_R$ growth direction, which corresponds to the [111] direction of the pseudo-cubic perovskite cell. The grain size for the $LaCoO_3$-850 layer is around 100 nm. Moreover, no cracks were observed in this layer. This triangular shape is lost for the $LaCoO_3$-1000 thin film (Fig. 2c), where grains still have flat termination but with irregular shapes, some of them being characteristic of a $[001]_R$ growth direction.

The topography of the surface was analyzed by AFM, carried out different area sizes, from 1 mm × 1 mm, to 100 nm × 100 nm. Selected results are presented on Fig. 3. The influence of deposition temperature is visible on the surface topography. For $LaCoO_3$-750, the surface is covered by small droplets (Fig. 3a). Similarly, the surface $LaCoO_3$-850 (Fig. 3b) contains droplets but larger and much less frequent. $LaCoO_3$-1000 is free from droplets (Fig. 3c).

The roughness parameters R_{max}, R_a and R_q, determined on regions free of droplets, are presented in Table 2.

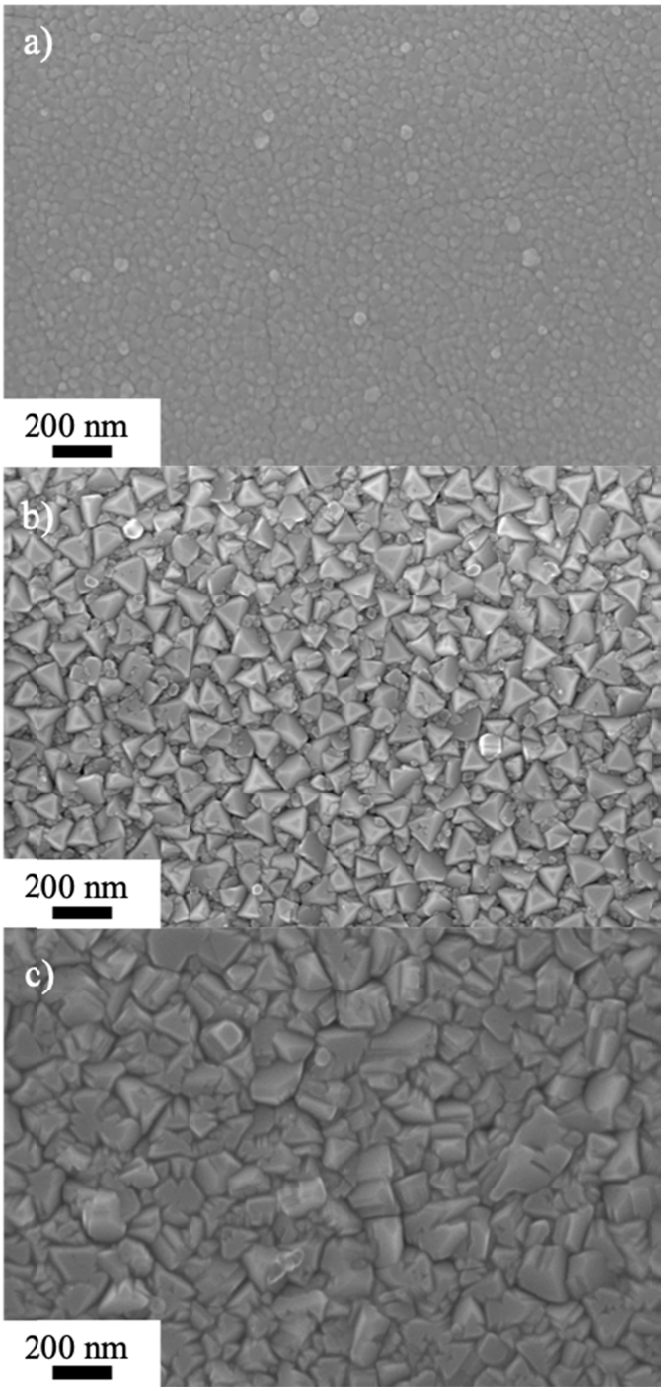

Fig. 2. $LaCoO_3$ surface a) $LaCoO_3$-750°C, b) $LaCoO_3$-850°, c) $LaCoO_3$-1000°C

TABLE 2

AFM results of $LaCoO_3$

Sample	R_a [nm]	R_{max} [nm]	R_q [nm]
$LaCoO_3$-750	1,27	16,5	1,67
$LaCoO_3$-850	1,54	11,9	1,92
$LaCoO_3$-1000	2,51	20,0	3,13

Thin films obtained at high temperatures are characterized by higher roughness parameters. The increase of R_a parameters is a consequence of the change in morphology and an increase of grain size.

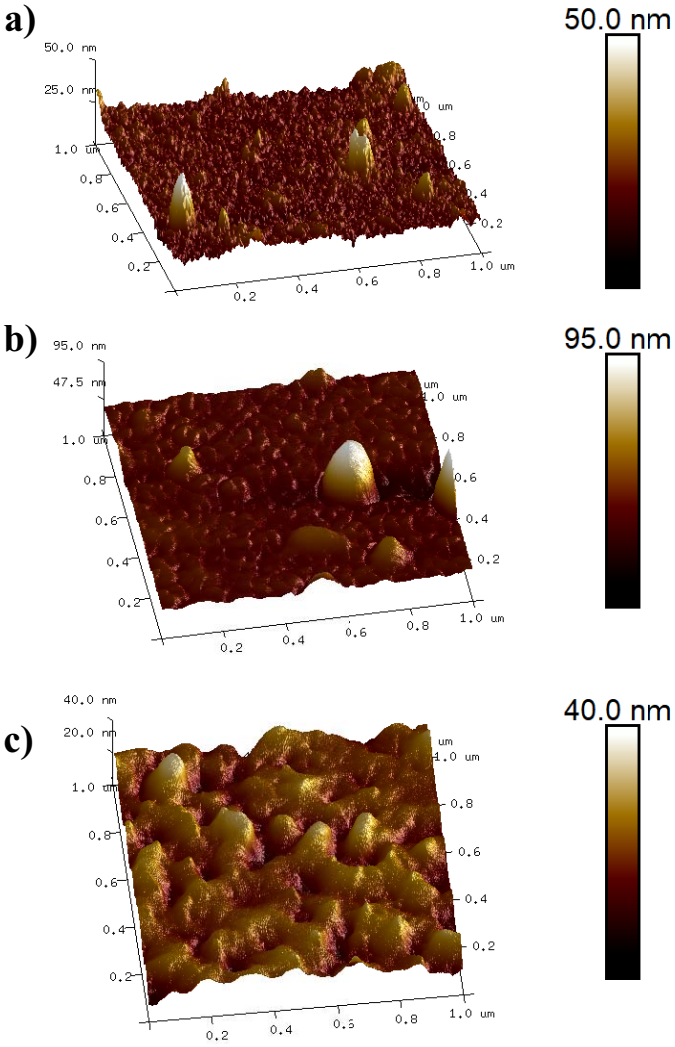

Fig. 3. $LaCoO_3$ surface a) $LaCoO_3$-750°C, b) $LaCoO_3$-850°, c) $LaCoO_3$-1000°C

In order to obtain information about the thickness of thin films and the grain growth, as well as chemical composition, TEM analysis coupled with EDS were performed on cross-sectional samples. EDS analysis showed that the films have a homogeneous composition. The quantification, using the $LaCoO_3$ target as standard, evidenced a deficiency in cobalt (see Table 3). This result is in accordance with the XDR results. EDS also confirms that the droplets and layers composition have the same chemical composition. This slight cobalt deficiency could be due to the low oxygen pressure (40 mTorr) in the deposition chamber [24].

TABLE 3

EDS results obtained on $LaCoO_3$-850

Element	Atomic %
La (L)	56
Co (K)	44

TEM results are summarized in Fig. 4. In all images, a native SiO_2 layer is visible between the $LaCoO_3$ film and the Si

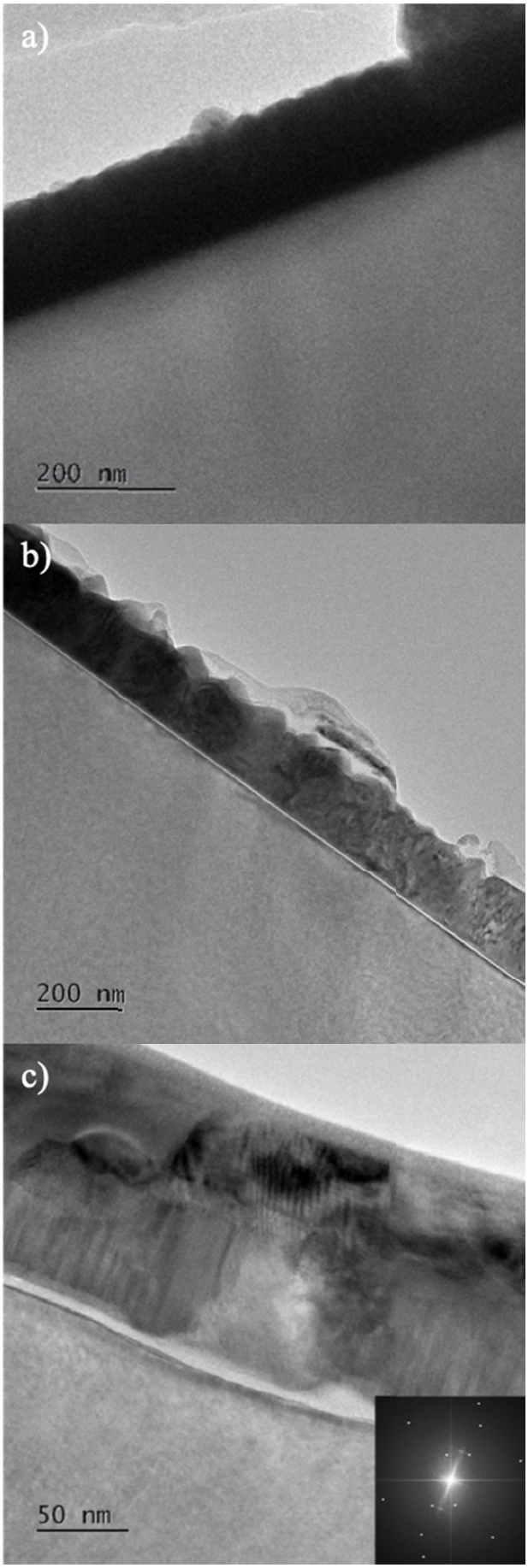

Fig. 4. TEM images of $LaCoO_3$ a) $LaCoO_3$-750, b) LaCoO3-850, c) $LaCoO_3$-1000

substrate. For $LaCoO_3$-750 and -850, the grain growth is columnar, with an average layer thickness of 170 nm (Fig. 4a & b). In Fig. 4a droplets are observed on top of the layer.

The roughness of the $LaCoO_3$-750 thin film seems rather low on TEM images, and a higher roughness is observed for $LaCoO_3$-850 (Fig. 4b), which is consistent with the AFM results.

Columns with regular triangular tips (75-100 nm) or a small flat termination can be observed; the lateral grain size varies from 75 nm to 100 nm. On the contrary, $LaCoO_3$-1000 exhibits a completely different morphology when observed in cross-section (Fig. 4c). The layer consists indeed of two distinct phases, one identified as La_2SiO_7 by high-resolution electron microscopy with distance d_{hkl} = 10.5 Å (see FFT in Fig. 4c), near the substrate, and a layer of $LaCoO_3$ grains on top. The presence of a La_2SiO_7 layer, 75-85 nm thick, indicates that at 1000°C, Si can diffuse through the native SiO_2 barrier and built a lanthanum silicate. Silicates were already observed in thin films obtained by PLD with a deposition temperature of 1100°C [25]. As XRD patterns were collected under grazing incidence, the depth penetration of X rays was insufficient to reach the $La_2Si_2O_7$ layer, which explains why no information about it was obtained by GIXRD. The $LaCoO_3$ grains grown on La_2SiO_7 have a different morphology than those grown on Si. This change in morphology is expected to have a strong effect on the sensing characteristic of the material.

4. Conclusion

The main objective of this research was to analyze the influence of substrate temperature during Pulsed Laser Deposition, on the structure and morphology of $LaCoO_3$ films, for gas sensor applications. The rise of deposition temperature leads to an increase in grain size and an elimination of droplets and cracks. Increase of the grain size (observed by SEM and TEM) and increase of the roughness parameter R_a determined by AFM might have a positive impact on the sensitivity to gases due to the increase of the surface exposed to the gas. A low temperature (750°C) leads to the presence of cracks and droplets. A high temperature deposition (1000°C) is causing creation of additional phase of La_2SiO_7 and a modification of the grain morphology. A temperature of 850°C seems to be the most suitable elaboration temperature for gas sensing applications. Indeed, it leads to the growth of nanosized columnar grains with a triangular shape, implying that specific crystallographic facets will be exposed to the gases. As expected, a proper selection of the temperature is necessary for the control of the morphology of $LaCoO_3$ thin layers obtained by PLD.

Further studies will be carried out to evaluate the gas sensing characteristics of these layers, starting with resistivity measurements under gas. These data will be produced in a future report.

Acknowledgements

This work was done in the general framework of the French-Polish PHC Polonium 40523VD exchange program. Authors acknowledge the Ph.D. scholarship of the French embassy in Poland.

REFERENCES

[1] N. Afifah, R. Saleh, Synthesis, Characterization and Catalytic Properties of Perovskite $LaFeO_3$ Nanoparticles, J. Phys. Conf. Ser. **710**, 012030 (2016).

[2] M. Johnsson, P. Lemmens, Crystallography and Chemistry of Perovskites, ArXivcond-Mat0506606, Jun. 2005.

[3] I.R. Shein, K.I. Shein, V.L. Kozhevnikov, A.L. Ivanovski, Band Structure and the Magnetic and Elastic Properties of $SrFeO_3$ and $LaFeO_3$ Perovskites, **47**, 11, 7 (2005).

[4] X. Yang, L. Yang, W. Fan, H. Lin, Effect of redox properties of $LaCoO_3$ perovskite catalyst on production of lactic acid from cellulosic biomass, Catal. Today **269**, 56-64 (2016).

[5] Q. Fan et al., Catalytic oxidation of diesel soot particulates over $Ag/LaCoO_3$ perovskite oxides in air and NO_x, Chin. J. Catal. **37**, 3, 428-435 (2016).

[6] K. Cvejin, M. Śliwa, L. Manjakkal, J. Kulawik, G. Stojanović, D. Szwagierczak, Impedancemetric NO sensor based on YSZ/perovskite neodymium cobaltite operating at high temperatures, Sens. Actuators B Chem. **228**, 612-624 (2016).

[7] Z. Duan, Y. Zhang, Y. Tong, H. Zou, J. Peng, X. Zheng, Mixed-Potential-Type Gas Sensors Based on Pt/YSZ Film/$LaFeO_3$ for Detecting NO_2, J. Electron. Mater. **46**, 12, 6895-6900 (2017).

[8] M. Enhessari, A. Salehabadi, Perovskites-Based Nanomaterials for Chemical Sensors, in Progresses in Chemical Sensor, W. Wang, Ed. InTech, 2016.

[9] W. Haron, A. Wisitsoraat, S. Wongnawa, Nanostructured perovskite oxides – $LaMO_3$ (M=Al, Co, Fe) prepared by co-precipitation method and their ethanol-sensing characteristics, Ceram. Int. **43**, 6, 5032-5040 (2017).

[10] I.-S. Hwang et al., Enhanced H_2S sensing characteristics of SnO_2 nanowires functionalized with CuO, Sens. Actuators B Chem. **142**, 1, 105-110 (2009).

[11] M. Radovic et al., Thermal, mechanical and phase stability of $LaCoO_3$ in reducing and oxidizing environments, J. Power Sources **184**, 1, 77-83 (2008).

[12] P.H.T. Ngamou, N. Bahlawane, Influence of the Arrangement of the Octahedrally Coordinated Trivalent Cobalt Cations on the Electrical Charge Transport and Surface Reactivity, Chem. Mater. **22**, 14, 4158-4165 (2010).

[13] J. Wang, Z. Yan, L. Liu, Y. Zhang, Z. Zhang, X. Wang, Low-temperature SCR of NO with NH_3 over activated semi-coke composite-supported rare earth oxides, Appl. Surf. Sci. **309**, 1-10 (2014).

[14] Z. Say et al., Palladium doped perovskite-based NO oxidation catalysts: The role of Pd and B-sites for NO_x adsorption behavior via in-situ spectroscopy, Appl. Catal. B Environ. **154-155**, 51-61 (2014).

[15] V. Chumakova, A. Marikutsa, M. Rumyantseva, D. Fasquelle, A. Gaskov, Nanocrystalline $LaCoO_3$ modified by Ag nanoparticles with improved sensitivity to H2S, Sens. Actuators B Chem. **296**, 126661, (2019).

[16] J.-C. Ding, H.-Y. Li, X. Guo, CO sensing mechanism of $LaCoO_3$, Solid State Ion. **272**, 155-159 (2015).

[17] L. Gildo Ortiz et al., Low-Temperature Synthesis and Gas Sensitivity of Perovskite-Type $LaCoO_3$ Nanoparticles, J. Nanomater. **2014**, 1-8 (2014).

[18] X. Yang, D.-W. Park, M.-I. Kim, Selective oxidation of hydrogen sulfide over $LaCoO_3$ and $LaSrCoO_4$ mixed oxides, Korean J. Chem. Eng. **24**, 4, 592-595 (2007).

[19] P.R.N. Silva, A.B. Soares, Lanthanum based high surface area perovskite-type oxide and application in CO and propane combustion, São Paulo, p. 8, 2009.

[20] M. Popa, J.M. Calderón-Moreno, Lanthanum cobaltite thin films on stainless steel, Thin Solid Films **517**, 5, 1530-1533 (2009).

[21] S. Skrzypek, Nowe możliwości pomiaru makronaprężeń własnych materiałów przy zastosowaniu dyfrakcji promieniowania X w geometrii stałego kąta padania, AGH Uczelniane Wydawnictwa Naukowo-Dydaktyczne, Kraków (2002).

[22] W. Wu, J.T. Cheung, Low temperature growth of epitaxial $La_{o.s}Sr_{o.s}CoO_3$ films on (100) $SrTiO_3$ by pulsed laser deposition," p. 4.

[23] M.D. Scafetta, S.J. May, Effect of cation off-stoichiometry on optical absorption in epitaxial $LaFeO_3$ films, Phys. Chem. Chem. Phys. **19**, 16, 10371-10376 (2017).

[24] R. Chmielowski, V. Madigou, M. Blicharski, Ch. Leroux, Sr-4Ru2O9 films grown by pulsed laser deposition Journal of Crystal Growth **310**, 3854-3860 (2008).

[25] A. Kopia, K. Kowalski, Ch. Leroux, J.R. Gavarri, Influence of the substrate on the structure stability $LaLuO_3$ thin films deposited by PLD method, Vacuum **134**, 120-129 (2016).